SLAC-PUB-12835
September 2007

The GeV-TeV Connection in galactic gamma-ray sources

S. Funk[1], O. Reimer[2], D. F. Torres[3], J. A. Hinton[4]

ABSTRACT

Recent observations by atmospheric Cherenkov telescopes such as H.E.S.S. and MAGIC have revealed a large number of new sources of very-high-energy (VHE) gamma-rays above 100 GeV, mostly concentrated along the Galactic plane. At lower energies (100 MeV – 10 GeV) the satellite-based instrument EGRET revealed a population of sources clustering along the Galactic Plane. Given their adjacent energy bands a systematic correlation study between the two source classes seems appropriate. While only a few of the sources connect, both in terms of positional coincidence and spectral consistency, most of the detections occur only in one or the other energy domain. In these cases, for the first time consistent upper limits in the other energy band have been derived. Here, the populations of Galactic sources in both energy domains are characterised on observational as well as on theoretical grounds, followed by an interpretation on their similarities and differences. The observational data at this stage suggest rather different major source populations at GeV and TeV energies. With regards to preparations for the upcoming GLAST mission that will cover the energy range bridging GeV and TeV instruments this paper investigates the connection between the population of sources in these bands and concludes with predictions for commonly observable sources for GLAST-LAT detections.

Subject headings:

---

[1]Kavli Institute for Particle Astrophysics and Cosmology (KIPAC) at Stanford, CA 94025, USA. funk@slac.stanford.edu

[2]Stanford University, W. W. Hansen Experimental Physics Lab (HEPL) and KIPAC, Stanford, CA 94305-4085, USA. olr@stanford.edu

[3]ICREA & Institut de Ciencies de l'Espai (IEEC-CSIC) Campus UAB, Fac. de Ciencies, Torre C5, parell, 2a planta, 08193 Barcelona, Spain. dtorres@aliga.ieec.uab.es

[4]School of Physics and Astronomy, University of Leeds, Leeds LS2 9JT, UK. jah@ast.leeds.ac.uk

Submitted to Astrophysical Journal

Work supported in part by US Department of Energy contract DE-AC02-76SF00515

1. Introduction

Recent years have greatly improved our knowledge of the VHE gamma-ray sky above 100 GeV through the detection and subsequent study of a wealth of sources mostly by means of ground-based Imaging Atmospheric Cherenkov telescopes such as the High Energy Stereoscopic System (H.E.S.S.) or the Major Atmospheric Gamma-ray Imaging Cherenkov Observatory (MAGIC). Previously unknown Galactic VHE gamma-ray emitters such as shell-type Supernova remnants (Aharonian et al. 2006a, 2007a,b), Pulsar Wind Nebulae (Aharonian et al. 2005a, 2006b,c), gamma-ray binaries (Aharonian et al. 2006d; Albert et al. 2006), Molecular clouds (Aharonian et al. 2006e) and possibly also star-forming regions (Aharonian et al. 2007c) were found both in pointed observations by H.E.S.S. and MAGIC as well as in a systematic survey of the inner Galaxy performed with the H.E.S.S. instrument. The maximum photon energies detected amongst this variety of source classes reaches $\sim$ 100 TeV (Aharonian et al. 2007a). Since these energies thus far represent the observable end of the electromagnetic spectrum for astrophysical objects, one immediate question concerns the connection and common aspects with sources at lower energies. The adjacent lower energy band has been studied by the Energetic Gamma Ray Experiment Telescope (EGRET) aboard the Compton Gamma-Ray Observatory with an energetic coverage between 100 MeV and 10 GeV (Hartman et al. 1999). At first glance, the GeV sky has a distinctively different appearance compared to the TeV sky. The most prominent feature of the GeV sky is the dominant diffuse emission from Cosmic Ray (CR) interactions in the Galactic plane, while the TeV sky is resolved into individual sources and is not dominated by diffuse emission due to the steeply falling energy spectrum of that emission. However, several prominent gamma-ray sources are known to emit gamma-rays both at GeV and at TeV energies, with the Crab Nebula being the best example (Weekes et al. 1989; Nolan et al. 1993; Aharonian et al. 2004, 2006f; Albert et al. 2007a).

In this paper the connection between EGRET sources and VHE gamma-ray sources will be assessed in a systematic way. For cases with a positional coincidence between a VHE and an EGRET source (in the following called "connecting sources") all currently known Galactic sources will be considered. For cases in which a source is detected only in one band – the "non-connecting sources" – the focus will be on the region covered during the H.E.S.S. Galactic plane survey (GPS) between 2004 and 2005 (Aharonian et al. 2005b, 2006g) (Galactic longitude $\pm 30^\circ$, Galactic latitude $\pm 3^\circ$) so a statistical assessment of the non-connection can be performed. EGRET was unable to perform detailed studies of the gamma-ray sky above 10 GeV mostly due to back-splash of secondary particles produced by high-energy gamma-rays that caused a self-veto in the monolithic anti-coincidence detector used to reject charged particles. The upcoming Gamma Ray Large Area Space Telescope (GLAST) Large Area Telescope (LAT) will not be strongly affected by this effect since the

anti-coincidence shield was designed in a segmented fashion (Moiseev et al. 2007). The GLAST-LAT mission will therefore for the first time fully bridge the gap between the energy range of EGRET and current VHE instruments. Part of the study presented here can thus be seen as preparatory for GLAST-LAT studies of sources in the largely unexplored energy band between 10 and 100 GeV.

Currently there are 22 VHE gamma-ray sources known in the Inner Galaxy reported from the 2004 and 2005 H.E.S.S. GPS. The third EGRET catalogue (Hartman et al. 1999) represents the companion to the VHE source catalogues at an energy threshold of 100 MeV (with best sensitivity between 150 and 400 MeV, depending on the gamma-ray source spectrum). It lists 271 sources, 17 of which are located within the H.E.S.S. GPS region. While the EGRET range currently represents the nearest energy band to VHE gamma-rays, an EGRET source detected all the way up to $\sim$ 10 GeV still leaves a rather unexplored energetic gap of roughly one decade before the VHE gamma-ray energy range at $\sim$ 100 GeV sets in (is should be noted in this regard that EGRET has some sensitivity beyond 10 GeV and Thompson, Bertsch & O'Neal (2005) reported the detection of $\sim$ 1500 photons above that energy with 187 of these photons being found within 1° of a source listed in the third EGRET catalogue). Comparing instrumental parameters of VHE instruments and EGRET there is a clear mismatch both in angular resolution as well as in sensitivity as can be seen in Figure 1. In a $\sim$ 5 hour observation (as a typical value in the GPS region) H.E.S.S. is about a factor of $\sim 50 - 80$ more sensitive (in terms of energy flux $E^2 dN/dE$) than EGRET above 1 GeV in the Galactic Plane for the exposure accumulated between 1991 and 1995 (corresponding to the third EGRET catalogue). Assuming a similar energy flux output in the two different bands this mismatch implies at first sight that H.E.S.S. sources are not readily detectable by EGRET. Conversely (again under the assumption of equal energy flux output), VHE gamma-ray instruments should be able to detect the majority of the EGRET sources as suggested by various authors (see e.g. Wang et al. (2005); Petry (2001)). In reality this naïve expectation can be wrong in Galactic gamma-ray sources for various reasons as will be discussed later in more detail: EGRET sources might indeed not emit the same energy flux in the VHE gamma-ray band but rather show cutoffs or breaks in the unexplored energy gap between EGRET and H.E.S.S. (as e.g. known for pulsars). Furthermore, H.E.S.S.-like instruments are typically only sensitive to emission on scales smaller than $\sim 1°$. If some of the EGRET sources are extended beyond 1° without a dominant central excess mimicking a point-source characteristic (not precluded given EGRET's poor angular resolution), current Imaging Cherenkov instruments might not be able to detect them since these sources would completely fill the field of view (FoV). In summary, it seems evident that it is both interesting in itself and that now with the upcoming GLAST launch is the proper time to study the connection between GeV and TeV emitters. This paper presents a comprehensive study

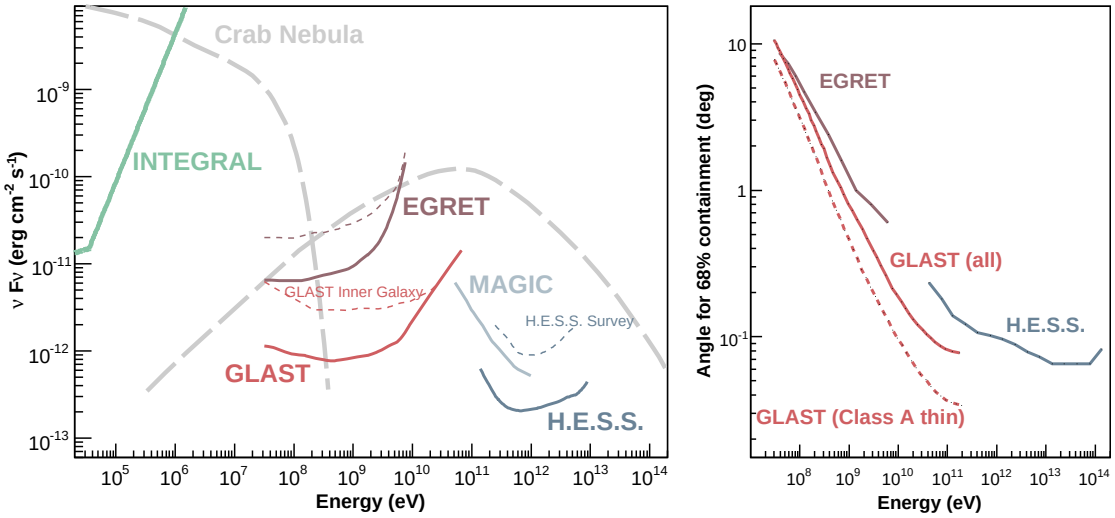

Fig. 1.— **Left:** Integral sensitivities for current and past gamma-ray instruments (5-σ sensitivity for $E > E_0$ multiplied with E_0 assuming a spectrum of E^{-2}). The solid lines show the nominal instrument sensitivities (for a typical observation time as specified below), the dashed curves show the actual sensitivities for the Inner Galaxy as appropriate for this work. INTEGRAL's (IBIS/ISGRI) sensitivity curve (solid green) shows the sensitivity for an observation time of 10^5s, a typical value in the Inner Galaxy. The EGRET curves (brown) are shown for the whole lifetime of the mission (periods 1–9) for the Galactic anti-center (solid) which received the largest exposure time and has a lower level of diffuse gamma-ray emission than the Inner Galaxy and for the position of RX J1713.7–3946 (dashed), a typical position in the Inner Galaxy dominated by diffuse gamma-ray background emission. The GLAST curves (red) show the 1-year sensitivity for the Galactic North pole (solid) – again a position with low diffuse emission and for the position of RX J1713.7–3946 (dashed). The H.E.S.S. curves (blue) are shown for a 50-hour pointed observation (solid) and for a 5-hour observation in the Inner Galaxy as typical for the Galactic Plane survey. The MAGIC curve (light blue) is shown for a 50-hour observation. **Right:** Energy-dependence of the angular resolution for current and past gamma-ray instruments expressed by the 68%-containment radius of the point-spread function (PSF). As can be seen, for high energies, the angular resolution of GLAST becomes comparable with current VHE instruments while at the low energy end GLAST and EGRET have comparable resolutions.

of these astrophysical sources at the top end of the electromagnetic spectrum. Section 2 describes the data and analysis methods used in this study, section 3 describes the sources detected in both energy bands, whereas section 4 focuses on sources only detected in one of

the two energy regimes. In section 5 astrophysical implications of the study will be drawn.

2. Analysis methods

For the sources discussed in this study, locations and source spectra in the EGRET band (Hartman et al. 1999) and in the VHE gamma-ray band have been used. For the inner Galaxy dedicated upper limits at the best fit position of the gamma-ray source in the respective other band were determined. For the EGRET data this upper limit (at 1 GeV) was derived at the nominal position of the H.E.S.S. sources based on a reanalysis of the data from the third EGRET catalogue by means of the standard EGRET likelihood fitting technique (Mattox et al. 1996). For the H.E.S.S. data, upper limits (2 σ) at the nominal position of an EGRET source were determined. This was done by scaling the flux corresponding to the H.E.S.S.-point-source sensitivity in 25 hours (1% of the Crab) by the ratio of 25 hours to the actual exposure time at the position of the EGRET source as published for the H.E.S.S. GPS region (Aharonian et al. 2006g).

2.1. Quantifying Positional Coincidence

One property of EGRET and VHE gamma-ray sources becomes immediately apparent in the investigation of source connections within the H.E.S.S. GPS region: only a minor fraction of the H.E.S.S. sources coincide within the considerably larger location uncertainty contours of EGRET GeV sources. Given the rather poor angular resolution of EGRET (68% containment radius of the PSF: 1.5° at 1 GeV) any systematic assessment of positional matches between EGRET and H.E.S.S. sources is dominated by the localisation error on the EGRET source position. The likelihood source location confidence contours as given in Hartman et al. (1999) have been used to check for VHE gamma-ray sources within these regions on the sky. While most of the VHE sources are extended, their extension is rather small on the scale of the EGRET positional uncertainty and therefore a source is classified as "connecting" if the centre of gravity of the VHE emission is within the EGRET positional uncertainty contour. For large sources such as e.g. the Supernova remnant (SNR) RX J1713.7–3946 (HESS J1713–395) this approach is clearly an oversimplification, albeit it is the one used at this stage of our study. The VHE gamma-ray emission in RX J1713.7–3946 and its connection to the close-by EGRET source 3EG J1714–3857 has been specifically treated recently in Aharonian et al. (2006a) where a reanalysis of the EGRET data has shown that no consistent picture can be found by assigning the EGRET photons to the VHE gamma-ray source. The upcoming GLAST-LAT instrument will shed more light on

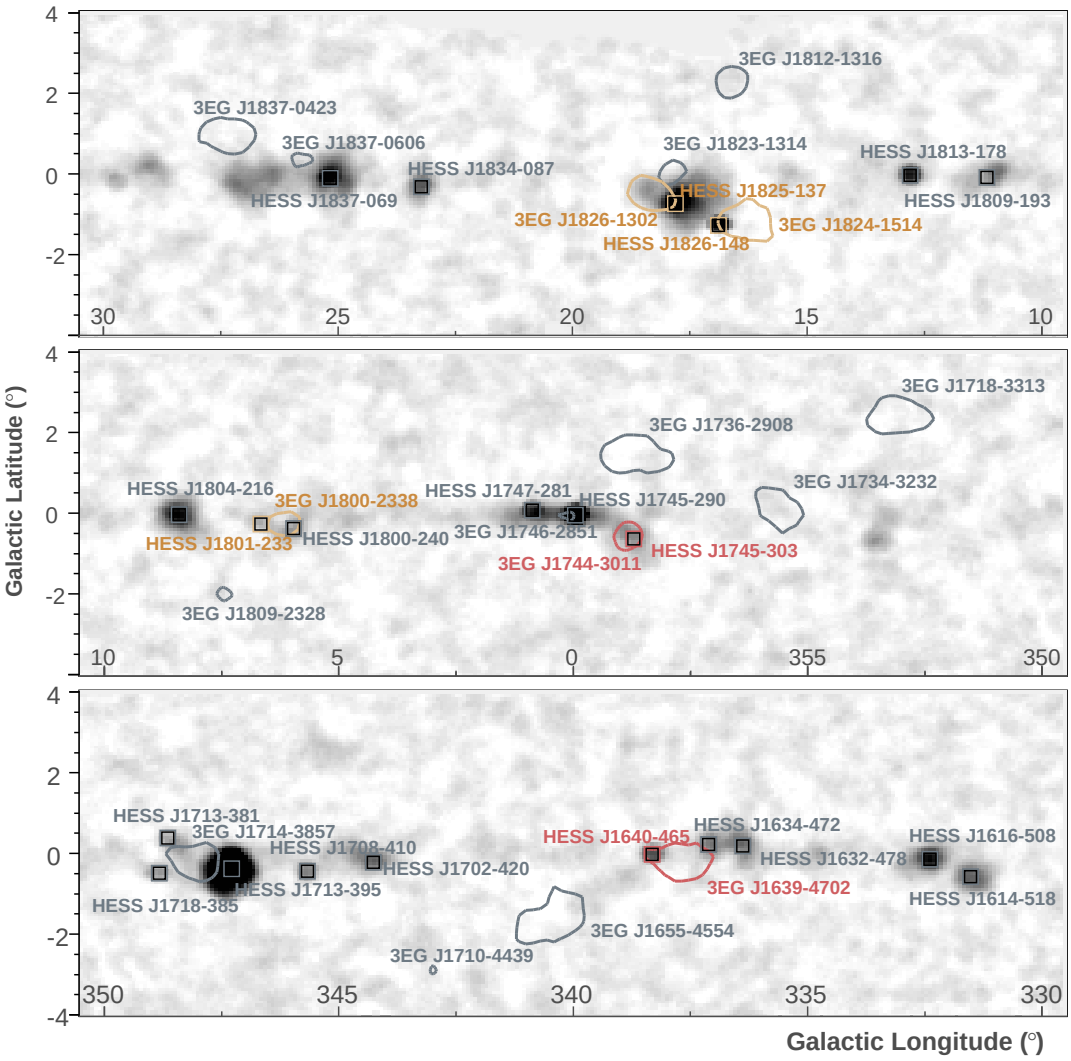

Fig. 2.— Significance map of the H.E.S.S. GPS region as published in Aharonian et al. (2006g) for the 2004–2005 data-set. Marked are all published H.E.S.S. sources (squares) and EGRET sources with their 95% positional confidence contours from the 3EG-catalogue. The red (orange) contours and labels denote connecting sources with a H.E.S.S. source located within the 95% (99%) confidence contour of an EGRET source.

this important source region as e.g. predicted in Funk et al. (2007b).

The number of spatially "connecting" sources depends on the EGRET source location uncertainty contour chosen to investigate the connection. For the H.E.S.S. GPS-region, not a single VHE gamma-ray source is located within any EGRET 68% positional confidence

EGRET Source	VHE gamma-ray Source		
	Within 68% Containment	Within 95% Containment	Within 99% Containment
	Within the H.E.S.S. GPS		
3EG J1639–4702		HESS J1640–465	
3EG J1744–3011		HESS J1745–303	
3EG J1800–2338	NONE		HESS J1800–233
3EG J1824–1514			HESS J1826–148
3EG J1826–1302			HESS J1825–137
	Outside the H.E.S.S. GPS		
3EG J0241+6103			MAGIC J0240+613
3EG J0617+2238		NONE	MAGIC J0616+225
3EG J0634+0521			HESS J0632+058
3EG J1420–6038	HESS J1420–607		

Table 1: Positionally coincident EGRET and H.E.S.S. sources depending on the 68%, 95%, and 99% positional uncertainty contour of the EGRET source both within and outside the H.E.S.S. GPS region.

contours. Relaxing the coincidence criterion, two VHE gamma-ray sources are located within the 95%-confidence contour of EGRET source positions (shown in red in Figure 2) and an additional three VHE gamma-ray sources are located within EGRET 99%-confidence contours (shown in orange in Figure 2). Outside the H.E.S.S. GPS-region, no systematic statistical assessment of the non-connecting sources is possible due to the patchy observation strategy of the limited-FoV VHE-instruments. Nevertheless, it should be noted that four additional connecting sources are found outside the H.E.S.S. GPS-region within the Galactic plane: in particular HESS J1420–608 (Aharonian et al. 2006c) in the Kookaburra region is located within the 68% confidence contour of 3EG J1420–6038. The other three connecting Galactic sources are located within the 99% confidence contours of EGRET sources (Hartman et al. 1999). All of these connecting cases will be discussed further in section 3. Table 1 summarises the VHE gamma-ray sources located within EGRET confidence contours inside and outside the H.E.S.S. GPS region. From the total sky coverage by EGRET sources within the GPS region of 3×10^{-3} sr (determined from elliptical fits to the 95% positional confidence contours (Mattox, Hartman & Reimer 2001)), corresponding to 3% of the total area of the GPS, a chance spatial coincidence is expected for ~ 0.6 source given the size of the H.E.S.S. sample. The probability of detecting 2 sources when 0.6 sources are expected by chance is

12%. Using the expected number of 0.6 sources determined from the 95% confidence contours and considering the additional 3 sources located within the 99% confidence contours, the probability for 5 positionally coincident sources is 0.04%. Summarising these numbers, a positional coincidence of 3 sources within the 95% contour level or even of 5 sources within the 99% confidence contours might occur by chance as indicated by the numbers shown here. When taking into account not the full ±3° Galactic latitude width of the H.E.S.S. GPS but a smaller region in which most of the H.E.S.S.-sources are concentrated the probability for chance coincidences will even increase accordingly.

2.2. Determining Spectral Match

Besides the test for positional coincidence a test of spectral compatibility, based on the simple assumption of a connection by a single power-law between the EGRET and the H.E.S.S.-range can be performed. To assess the spectral match the quantity σ_{comb} has been defined in the following way:

$$\sigma_{\mathrm{comb}} = \sqrt{\sigma_{\mathrm{3EG}}^2 + \sigma_{\mathrm{H.E.S.S.}}^2} \tag{1}$$

To determine σ_{3EG}, the spectral index of the EGRET source has been varied (around the pivot point of the EGRET best fit) until the extrapolation to 1 TeV matches the H.E.S.S. flux at that energy. This index is called Γ_{match} and

$$\sigma_{\mathrm{3EG}} = (\Gamma_{\mathrm{match}} - \Gamma_{\mathrm{3EG}})/(\Delta\Gamma_{\mathrm{3EG}}) \tag{2}$$

(where Γ_{3EG} and $\Delta\Gamma_{\mathrm{3EG}}$ is the EGRET index and its error taken from Hartman et al. (1999)). Consequently, σ_{3EG} is a quantity that describes by how much the EGRET index has to be altered (with respect to the error on this index) to match the H.E.S.S. spectrum at 1 TeV. In the same way $\sigma_{\mathrm{H.E.S.S.}}$, is determined by changing the H.E.S.S. spectral index until the flux matches the EGRET flux at 1 GeV (to avoid biases through spectral cutoffs at the high end of the H.E.S.S. energy range the spectra were fitted only below 1 TeV in cases with obvious cutoffs). The two quantities σ_{3EG} and $\sigma_{\mathrm{H.E.S.S.}}$ are finally added in quadrature to yield σ_{comb}, describing how well the two spectra can be connected into each other by a linear extrapolation (see equation 1). It should be noted that for the procedure described here, only the statistical (not the systematic) errors on the spectral indices are taken into account. For cases with a source detection only in one band, the same procedure can be applied using the upper limit in the other band (with the obvious difference that only the extrapolation from the source spectrum onto the upper limit can be performed, not the other way around). For cases in which the power-law extrapolation with the nominal source photon index turns out

to be lower – and therefore non-constraining – to the upper limit the corresponding measure $\sigma_{\rm 3EG}$ or $\sigma_{\rm H.E.S.S.}$ is set to zero (i.e. the spectra are compatible). In several (but not the majority of) cases the EGRET spectrum can be preferentially fit by a higher order spectral shape (e.g. a exponential cutoff or a broken power-law) as will be discussed in section 4.

3. VHE gamma-ray sources with EGRET counterparts

Only a few connecting sources between the GeV and the TeV band have been reported so far. The VHE gamma-ray sources that positionally coincide with EGRET sources are summarised in Table 1. While a chance coincidence between EGRET and VHE gamma-ray sources is possible as shown in the previous section, in the following all positional coincidences within the 99% EGRET positional confidence region will be considered. Some of the properties of the sources and their respective source classes will be discussed along with an investigation on their spectral compatibility as introduced in the previous section.

3.1. Source Classes

For EGRET sources in the Galactic plane, only pulsars have been firmly identified based on the matching radio or X-ray periodicity of the emission (Thompson et al. 1994). For many of the remaining Galactic EGRET sources counterparts have been suggested, but the angular resolution of the instrument and the strong diffuse gamma-ray background in the Galactic plane prevented an unambiguous identification. In VHE gamma-rays several source classes have been firmly identified as has been discussed in e.g. Funk (2006), based on matching morphology, positional coincidence or periodicity. However, the majority of Galactic VHE gamma-ray sources remains unidentified as well. Table 2 summarises potential counterparts of VHE source in the connecting cases. While some of these identifications are rather solid (as e.g. in the case of the gamma-ray binaries LS 5039 (Aharonian et al. 2006d) and LSI +61 303 (Albert et al. 2006)), in most of the other cases the identification of (even) the VHE gamma-ray source (which is measured with relatively high position resolution of $\sim 1'$) lacks a firm proof beyond the sheer positional match. In case of a firm identification, the VHE gamma-ray source can be used to shed light on a GeV source assuming a connection between the VHE gamma-ray and the GeV source as shown exemplary for the Kookaburra region (Reimer & Funk 2007). In that source region high-angular resolution VHE gamma-ray data taken with H.E.S.S. (Aharonian et al. 2006c) provided a template for the re-analysis of the EGRET data in which the GeV source (flagged as "confused" in the 3rd EGRET catalogue (Hartman et al. 1999)) was found to follow the morphology suggested by the TeV

emission. Such studies demonstrate that observations with VHE gamma-ray instruments can provide necessary templates to pinpoint the nature of intriguing and promising but still unidentified EGRET gamma-ray sources. With the upcoming advent of the GLAST-LAT instrument this approach will become very useful for connecting the GeV emission as measured by a large-aperture space-based gamma-ray instrument with narrow FoV but superior spatial resolution observations of ground-based VHE gamma-ray instruments. Provided that the connections discussed in this section and shown in Table 2 are confirmed (as e.g., through the more sensitive GLAST-LAT measurements), three long-suspected new source classes could finally conclusively be established as Galactic GeV emitters. In the following we will briefly discuss these different source classes in the context of our study.

EGRET source	VHE gamma-ray source	Potential Counterpart
Within the H.E.S.S. GPS		
3EG J1639–4702	HESS J1640–465	G338.3–0.0 (SNR/PWN)
3EG J1744–3011	HESS J1745–303	
3EG J1800–2338	HESS J1801–233	W28 (SNR)
3EG J1826–1302	HESS J1825–137	G18.0–0.7 (PWN)
3EG J1824–1514	HESS J1826–148	LS 5039 (Binary)
Outside the H.E.S.S. GPS		
3EG J0241+6103	MAGIC J0240+613	LSI +61 303 (Binary)
3EG J0617+2238	MAGIC J0616+225	IC443 (SNR/PWN)
3EG J0634+0521	HESS J0632+058	Monoceros
3EG J1420–6038	HESS J1420–607	Kookaburra (PWN)

Table 2: Connecting sources and potential counterpart to the VHE gamma-ray source (and therefore also to the EGRET source). The counterparts are classified into source classes such as shell-type Supernova remnants (SNR), Pulsar Wind Nebulae (PWN) and gamma-ray binaries.

3.1.1. Pulsar wind nebulae

Pulsar wind nebulae are currently the most abundant among the identified Galactic VHE gamma-ray sources, therefore it is not surprising that prominent PWN are found as potential counterparts to the connecting sources. The first example for connecting PWN is HESS J1825–137 – located within the 99% confidence region of 3EG 1826–1302. This source is currently the best example for an offset VHE gamma-ray PWN (Aharonian et al. 2006b)

and as such represents a prototype for a new class of VHE gamma-ray sources. HESS J1825–137 shows a steepening of the energy spectrum with increasing distance from the central pulsar. This property, as well as the observed difference in sizes between the VHE gamma-ray emitting region and the X-ray PWN associated with the pulsar PSR B1823–13 can be naturally explained by different cooling timescales for the radiating electron populations. In this regard it will be important to study this region with the high sensitivity of the GLAST-LAT in the GeV band to confirm this picture. Another example for a VHE gamma-ray PWN is the previously discussed Kookaburra source located within the 68% confidence region of 3EG J1420–6038. The Crab Nebula is not listed in Table 2 although it has been detected by EGRET (Nolan et al. 1993) as well as by all major VHE Gamma-ray instruments (Weekes et al. 1989; Atkins et al. 2003; Aharonian et al. 2004, 2006f; Albert et al. 2007a). The reason for this is that in the 3EG catalogue only the position of the Crab pulsar is given, whereas the uncertainty contour of the off-pulse emission (i.e. the Nebula emission) has not been published thus far. For some of the other connecting sources such as HESS J1640–465 (G338.3–0.0) or MAGIC J0616+225 (IC443) (Albert et al. 2007b) an association with the X-ray PWN detected in these systems (Funk et al. 2007; Gaensler et al. 2006) is suggestive but not firmly established at this point.

3.1.2. Shell-type Supernova remnants

Shell-type SNRs constitute another prominent source class of VHE gamma-rays. It is interesting to note, that the two most prominent VHE gamma-ray shell-type SNRs RX J1713.7–3946 and RX J0852.0–4622 (Vela Jr.) are not prominent GeV emitters even though they are (up to now) the brightest steady VHE gamma-ray sources in the sky besides the Crab Nebula. Also Cas A and RCW 86 have been reported as VHE gamma-ray sources (Aharonian et al. 2001; Albert et al. 2007c; Hoppe et al. 2007) but have not been detected by EGRET. Sturner & Dermer (1995); Esposito et al. (1996); Romero, Benaglia, & Torres (1999); Torres et al. (2003) assessed the potential connection between unidentified EGRET sources at low Galactic latitude and SNRs and found a statistically significant correlation between the two populations at the 4–5 σ level, were however not able to firmly and uniquely identify individual SNRs as EGRET sources. The GLAST-LAT will shed more light on the GeV emission in this source as well as in the whole population of Galactic Supernova remnants. By measuring the shape of the high-energy gamma-ray emission the GLAST-LAT might allow for a distinction between hadronic and leptonic emission models as discussed in section 5. Other potential shell-type SNR counterparts related to this analysis are W28 (HESS J1801–233 and 3EG J1800–2338) and Monoceros (HESS J0632+058 and 3EG J0634+0521), although in particular in the latter case, the morphology of the VHE gamma-ray source does not support

a connection to the Supernova remnant shell.

3.1.3. Gamma-ray binaries

Three prominent gamma-ray binary systems PSR B1259–63, LS 5039 and LSI +61 303 have been established as VHE gamma-ray sources (Aharonian et al. 2005c, 2006d; Albert et al. 2006; Smith et al. 2007) and at least the latter two of these objects have long been considered connected to EGRET sources (Kniffen et al. 1997; Tavani et al. 1998; Hartman et al. 1999; Paredes et al. 2000), however, a definite proof of identification could not be achieved in the GeV waveband so far. The VHE gamma-ray emission is undoubtedly connected to the binary system (as e.g. in LS 5039 established through the detection of characteristic periodicity, matching the orbital period of the binary system), which suggests that the GeV emission might also be connected to the binary system. Recently the MAGIC collaboration published a report on an indication of gamma-ray emission from the black-hole X-ray binary Cyg X-1 in a flaring state (Albert et al. 2007d). No EGRET emission has been reported from this object

3.2. Spectral connection

As described in section 2.2, a test for a compatibility between EGRET and H.E.S.S. energy spectra based on a single power-law extrapolation has been performed, calculating for each of the connecting cases in the H.E.S.S. GPS region the measure of spectral mismatch $\sigma_{\rm comb}$. Figure 3 shows the result of these extrapolations. The values for $\sigma_{\rm comb}$ are rather small, in particular if comparing to the positionally non-connecting sources that will be discussed in section 4. The largest value, potentially indicative of a spectral mismatch, is found for the case of the gamma-ray binary association LS 5039 (3EG J1824–1514 and HESS J1826–148). However, this value is completely dominated by the small statistical error on the H.E.S.S. power-law fit below 1 TeV (error on the photon index: $\Delta\Gamma_{\rm stat} = \pm 0.04$). Taking a typical H.E.S.S. systematic error of $\Delta\Gamma_{\rm sys} = \pm 0.2$ on the determination of the photon index Γ into account, the GeV and TeV energy spectra in this source match well. The trend that is evident in Figure 3, in particular, if comparing to the sources detected in one energy band (shown in the next section) is that the energy spectra of the sources that show a spatial association, can generally rather well be connected through a simple power-law extrapolation.

To estimate the chance coincidence of a spectral connection the spectra of all 17 EGRET sources and of all 22 H.E.S.S. sources in the H.E.S.S. GPS region have been interchanged

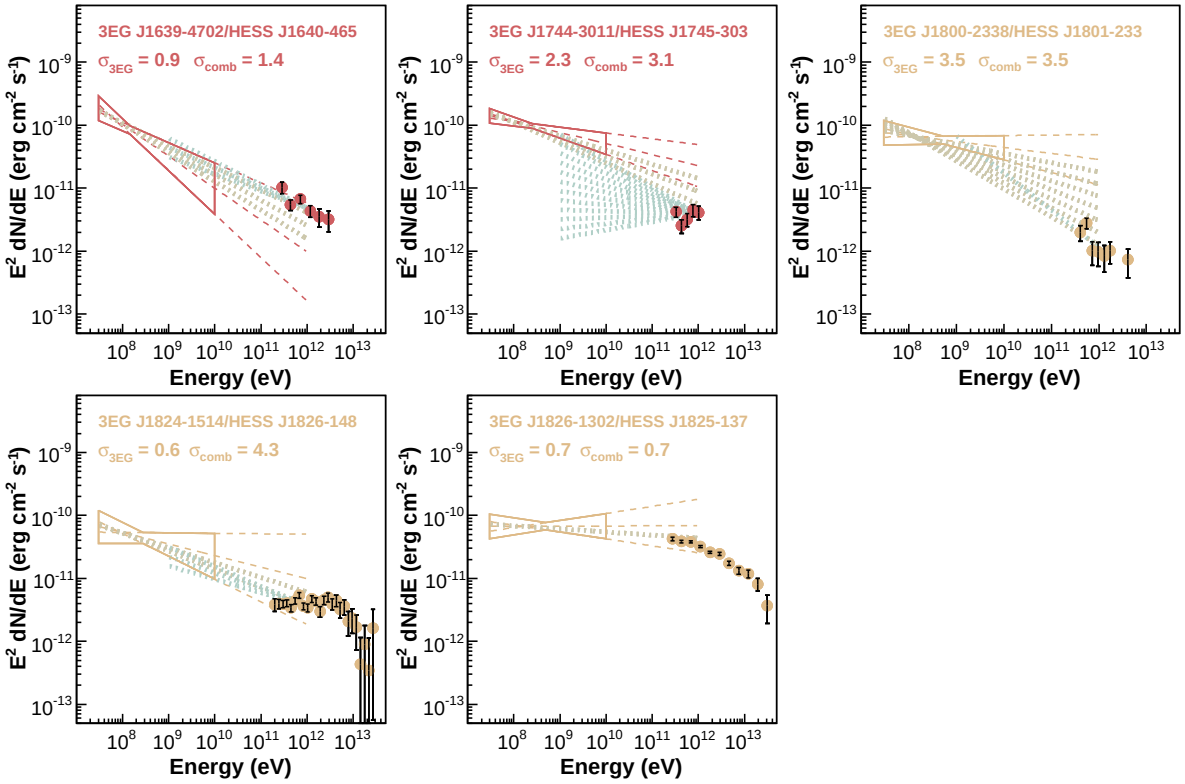

Fig. 3.— Spectra for the connecting EGRET and H.E.S.S. sources within the H.E.S.S. GPS region. Sources for which the H.E.S.S. source is located within the 95% confidence level are shown in red, whereas those within the 99% confidence contour (as give in Table 1) are shown in orange. The EGRET "butterfly" is determined from the 3EG catalogue (Hartman et al. 1999), the H.E.S.S. spectral points from the already cited respective publication. For HESS J1826–148 and HESS J1825–137 both showing signs for a cutoff in the energy spectrum, only the spectral points below 1 TeV have been fitted. Larger values of $\sigma_{\rm comb}$ point to stronger mismatches between the spectral shape at GeV and at TeV energies.

and "connected" to each other (i.e. each H.E.S.S. source has been connected to each EGRET source). The resulting distribution of $\sigma_{\rm comb}$ for these scrambled sources as shown in Figure 4 (red histogram) can be compared to the 5 cases in which a real connection (based on the positional coincidence) is expected. Even though the distribution for the scrambled sources shows a tail to values of $\sigma_{\rm comb}$ larger than 5, a Kolmogorov test yields a probability of 89% that the two distributions are based on a common underlying distribution. Thus a spectral match based on a power-law extrapolation of a typical (randomly picked) EGRET and a typical H.E.S.S. source can be expected to occur by chance regardless of the underlying reason. This is not surprising, given that both EGRET as well as H.E.S.S. spectra have

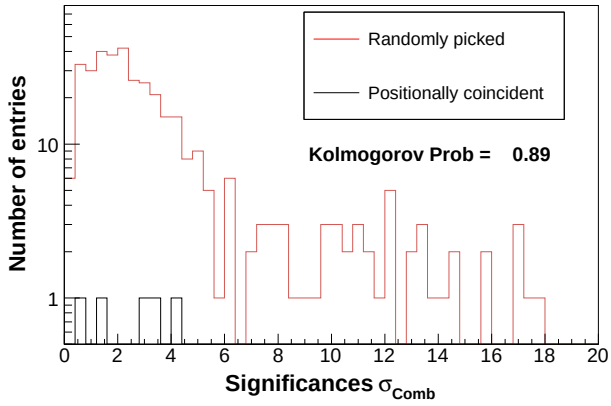

Fig. 4.— Distribution of $\sigma_{\rm comb}$. The red histogram shows the distribution for the spectral connectivity $\sigma_{\rm comb}$ of all combinations EGRET sources with H.E.S.S. sources in the H.E.S.S. GPS region whereas the black histogram shows the same distribution for the 5 cases of positional coincidences.

typical photon indices ~ 2.2 and that H.E.S.S. measuring 1–2 orders of magnitude higher in energy is 1–2 orders of magnitude more sensitive. Nevertheless, the approach shown here will prove useful in the assessment whether an individual EGRET source a cutoff is needed to explain the non-detection by H.E.S.S. as will be discussed in the next section. The general trend that spatially connecting sources show also a spectral matches suggests that some of the connecting cases are real associations.

4. VHE gamma-ray sources and EGRET source in the Inner Galaxy detected only in one band

In this section the remainder (and majority) of sources in the H.E.S.S. GPS region will be discussed. These are the sources which do not have a counterpart in the neighbouring energy band. In Section 4.1 EGRET sources without a VHE gamma-ray counterpart will be discussed, section 4.2 investigates VHE gamma-ray sources without an EGRET counterpart.

4.1. EGRET sources without a VHE gamma-ray counterpart

Here we address those EGRET sources for which no VHE gamma-ray source was reported within their respective 99%-confidence contour. This sample consist of 12 EGRET

EGRET Source	H.E.S.S. Upper Limit (10^{-12} ergs cm^{-2} s^{-1})	$\sigma_{\rm comb}$
3EG J1655-4554	0.4	1.3
3EG J1710-4439	1.5	16.3
3EG J1714-3857	0.2	1.5
3EG J1718-3313	1.0	0
3EG J1734-3232	0.6	1.4
3EG J1736-2908	0.3	3.5
3EG J1746-2851	0.2	15.7
3EG J1809-2328	0.5	6.4
3EG J1812-1316	2.1	1.0
3EG J1823-1314	0.4	0
3EG J1837-0423	0.6	0
3EG J1837-0606	0.4	5.5

Table 3: EGRET sources without a VHE gamma-ray counterpart in the H.E.S.S. GPS region. The H.E.S.S. differential upper limits (2 σ) at 1 TeV for a point-source analysis are derived from data taken in 2004 and 2005 by translating the H.E.S.S. sensitivity to the respective H.E.S.S. exposure at the nominal EGRET position as described in the text.

detections, with E > 100 MeV fluxes ranging between 0.4 and 3.1 $\times 10^{-6}\,{\rm cm}^{-2}\,{\rm s}^{-1}$ and photon indices of the power-law fits between $\sim$1.75 and 3.2. For these 12 EGRET sources upper limits (2 σ) on the VHE emission at the nominal position of the EGRET source were determined at 1 TeV by scaling the H.E.S.S. sensitivity for a 5 σ point source detection (1% of the Crab in 25 h) to the actual exposures as published for the H.E.S.S. GPS region (Aharonian et al. 2006g). As previously described, a measure of the spectral non-connection $\sigma_{\rm 3EG}$ was determined by varying the EGRET photon index Γ around the pivot point of the "butterfly" until matching the H.E.S.S. upper limit at 1 TeV and then comparing this photon index to the photon index $\Gamma_{\rm 3EG}$ and its error $\Delta\Gamma_{\rm 3EG}$ from the 3EG catalogue (Hartman et al. 1999) as given in Equation 2. For cases in which the EGRET extrapolation with the nominal 3EG photon index undershoots the H.E.S.S. upper limit, $\sigma_{\rm 3EG}$ is set to zero. The resulting plots are shown in Figure 5.

In seven of the twelve cases the H.E.S.S. upper limit does not impose strong constraints on an extrapolation from the EGRET spectrum ($\sigma_{\rm 3EG} < 1.5$), particularly for EGRET sources with steep energy spectra. For the remaining five sources a H.E.S.S. detection could have been expected based on a naïve power-law extrapolation. In particular the

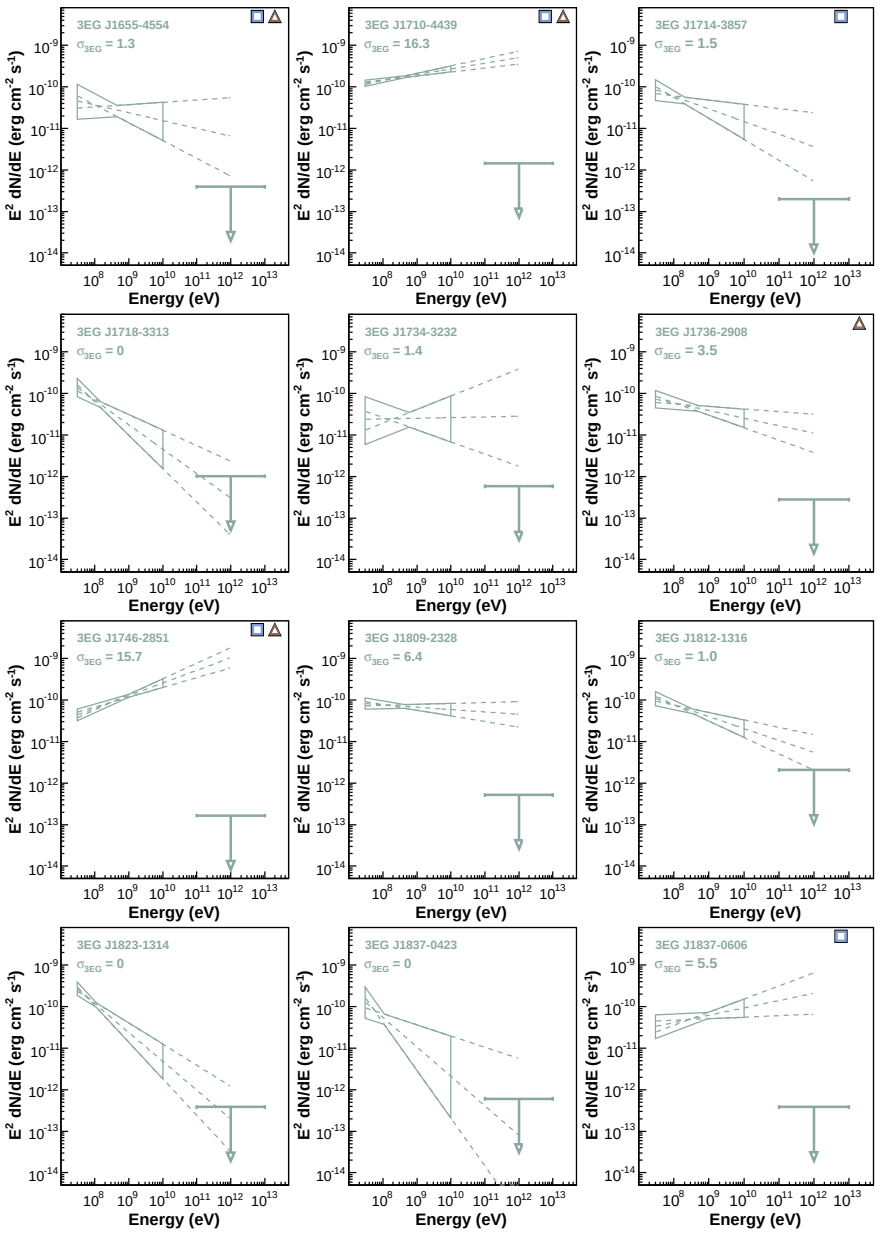

Fig. 5.— Spectral energy distribution of the EGRET source for which no VHE gamma-ray source was found within the 99% confidence contour. Sources marked with a blue-white square show gamma-ray emission above 10 GeV in the EGRET data as reported by Thompson, Bertsch & O'Neal (2005), for sources marked with a brown-white triangle the EGRET data can be better fitted with either a broken power-law or with an exponential cutoff as shown in Figure 6.

hard spectrum EGRET sources 3EG J1710–4439, 3EG J1746–2851, 3EG J1809–2328, and 3EG J1837–0606 appear to be incompatible with the H.E.S.S. upper limit at levels exceeding $\sigma_{3EG} > 5$. For these cases the VHE gamma-ray data strongly suggest some spectral turnover (cutoff or break) below the H.E.S.S. range. Such behaviour is not surprising for a variety of Galactic sources. For the EGRET-detected pulsars a cutoff in the energy spectrum is seen in many sources already in the EGRET energy regime (and therefore well below e.g. the H.E.S.S. range). In fact, for three out of the four EGRET sources for which a spectral change is suggested by the H.E.S.S. non-detection, a pulsar association has been proposed: 3EG J1710–4439 was unambiguously identified with PSR 1706–44 (Thompson et al. 1994), 3EG J1809–2328 was proposed to be of PWN nature (Braje et al. 2000), and 3EG J1837–0606 was suggested as counterpart of PSR J1837–0604 (D'Amico et al. 2001). The remaining source in the sample for which the spectral extrapolation of the EGRET source is constrained by the H.E.S.S. upper limit, is the Galactic centre source 3EG J1746–2851 too complex in the various rather different emission scenarios to be comprehensively treated here.

It is interesting to note, that an analysis of the EGRET data to search for events above 10 GeV (Thompson, Bertsch & O'Neal 2005) suggested a total of eleven EGRET sources showing emission above 10 GeV (at a level of less than 10% probability that the number of photons seen is a fluctuation of the diffuse emission). Five of these sources are located in the H.E.S.S. GPS region. These sources are 3EG J1655–4554, 3EG 1710–4439 (PSR B1706–44, showing a signal of 6.1σ detection significance above 10 GeV) 3EG J1714–3857, 3EG J1746–2851, and 3EG J1837–0606 (all of them marked with a white-and-blue square in Figure 5). Interestingly, all of these sources belong to the class of the non-connecting sources, i.e. have no counterpart at VHE gamma-ray energies. This emphatically emphasises the existence of cutoffs within the energetic gap left between the end of the EGRET measurements and the onset of the H.E.S.S. and MAGIC observations.

To further investigate the cutoff hypothesis a spectral analysis of the EGRET energy spectra has been performed by means of higher order representations as reported by Bertsch et al. (2000); Reimer & Bertsch (2001). The EGRET spectra were fitted with a broken power-law and with a power-law with exponential cutoff of the following forms:

$$\frac{\partial J}{\partial E}(E, K, \lambda_1, \lambda_2) = \begin{cases} K \left(\frac{E}{1\mathrm{GeV}}\right)^{-\lambda_1} (E \leq 1\mathrm{GeV}) \\ K \left(\frac{E}{1\mathrm{GeV}}\right)^{-\lambda_2} (E \geq 1\mathrm{GeV}) \end{cases} \tag{3}$$

$$\frac{\partial J}{\partial E}(E, K, \lambda, E_c) = K \left(\frac{E}{300\mathrm{MeV}}\right)^{-\lambda} exp\left(-\frac{E}{E_c}\right) \tag{4}$$

The resulting fits were then compared to the single power-law fit by the resulting χ^2 and

ultimately using an F-test to decide if there is sufficient statistical weight for the transition from a single power law fit to a higher order functional form. Several of the gamma-ray sources could not be tested for higher order functional fits due to insufficient data above the chosen break or cut-off energy. However, for four of the 17 EGRET sources considered in this study the F-test strongly suggests a different spectral form (by a probability value < 0.05 as discussed in detail in Reimer & Bertsch (2001)): 3EG J1655–4554 is better fit by a power-law with exponential cutoff, 3EG J1710-4439, 3EG J1736-2908, and 3EG J1746-2851 are best fit with a broken power-law. All of these sources have no positional counterpart at TeV energies (marked with triangles in Figure 5). The different spectral representations are shown in yellow in Figure 6. It is interesting to note, that out of the four sources mentioned above for which the H.E.S.S. non-detection strongly suggests a cutoff in the energy spectrum, the two sources with the largest incompatibility measure $\sigma_{\rm 3EG}$ are also characterised by a statistically significant cutoff in the EGRET spectrum. In particular, the previously mentioned source 3EG J1746–2851 (Galactic Centre) shows strong indications for an energy break below 10 GeV. In that respect, the anticipation of spectral changes (softening/cutoff) for compatibility with H.E.S.S. upper limit can be substantiated into observational constraints at both the GeV and the TeV energies: The indicated cutoff in some of the EGRET spectra corresponds nicely to the expected spectral changes from of the constraining VHE limit based on power-law extrapolation. The prediction that the other two EGRET sources (3EG J1809–2328, and 3EG J1837–0606) constrained by the H.E.S.S. upper limits show a cutoff in the energy range between 10 GeV and 100 GeV is therefore well justified and will readily be tested by upcoming GLAST-LAT observations.

4.2. VHE gamma-ray sources without an EGRET counterpart

In this section the H.E.S.S. sources without a catalogued EGRET counterpart are addressed. At all nominal H.E.S.S. source location flux upper limits have been determined from the EGRET data at energies above 1 GeV by means of the EGRET likelihood technique (Mattox et al. 1996). In the determination of the EGRET upper limit both the Galactic diffuse emission as well as point-sources exceeding a 5 σ-detection significance threshold were modelled and subsequently subtracted. The underlying EGRET exposure corresponds to the first four years of the EGRET mission. As previously discussed, the sensitivity of EGRET (in terms of energy flux E^2dN/dE) is considerably worse than the H.E.S.S. sensitivity so no EGRET detection of a H.E.S.S. source is expected under the assumption of equal energy flux. This assumption, however, is obviously not necessarily fulfilled in an astrophysical source.

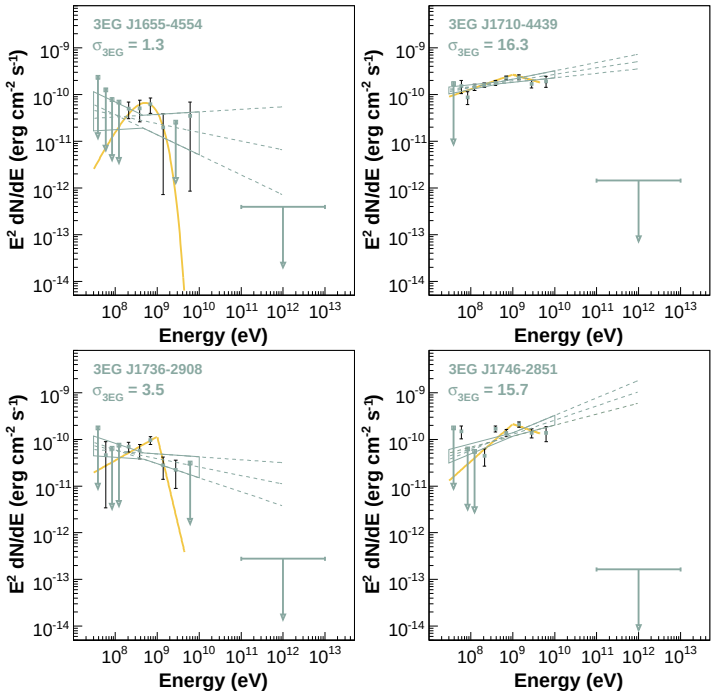

Fig. 6.— Spectral energy distribution at E > 30 MeV for the non-connecting cases in which the EGRET spectrum shows significant deviation from a simple power-law form. The previously reported higher order spectral representations are shown in yellow (exponential cutoff for 3EG J1655–4554 and broken power-law for 3EG J1710–4439, 3EG J1736–2908 and 3EG J1746–2851).

Methodologically similar to the previous section, the determination of spectral incompatibility was performed by extrapolating H.E.S.S.-measured VHE spectra to 1 GeV and comparing the resulting flux to the EGRET upper limit at that energy. The measure $\sigma_{\mathrm{H.E.S.S.}}$ is determined in a similar way as σ_{3EG} as previously described. In order to avoid biases by extrapolating H.E.S.S. spectra with apparent high-energy cutoffs, those were only fitted from the threshold energy at $\sim$ 100 GeV to 1 TeV. As in previous sections, $\sigma_{\mathrm{H.E.S.S.}}$ describes how well the extrapolated H.E.S.S. spectrum can be accommodated by the EGRET upper limit. The resulting spectral energy distributions for the non-connecting H.E.S.S. sources are shown in Figures 7 and 8.

In all cases, the values of $\sigma_{\mathrm{H.E.S.S.}}$ are less then or equal to 1, implying that no EGRET upper limit is violated by the H.E.S.S. extrapolation to 1 GeV. In stark contrast to the results discussed in the previous section, there are consequently no constraints from the EGRET upper limits based on our assumption of single power-law extrapolation. The most interesting

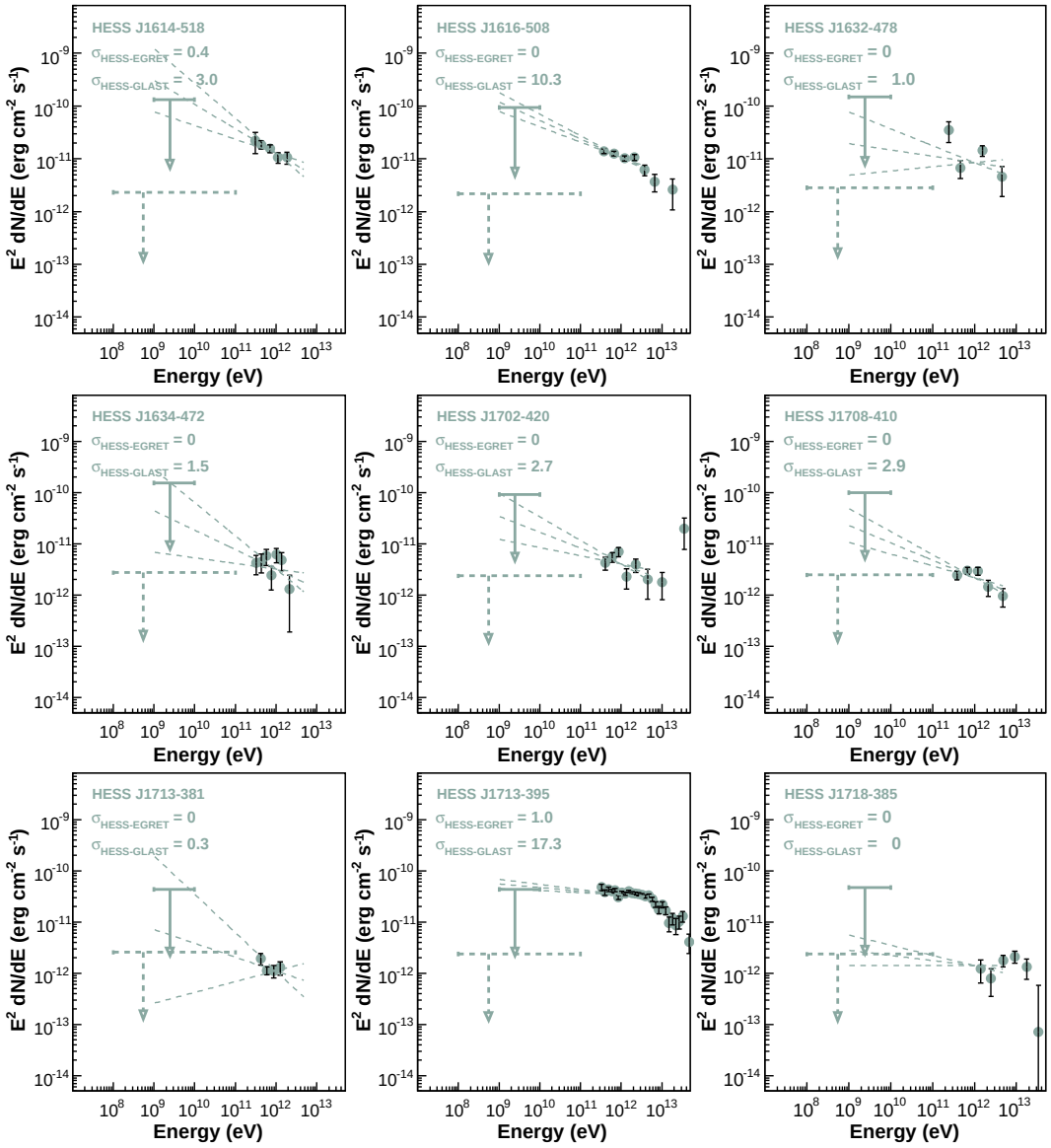

Fig. 7.— (Part 1) Spectral energy distribution at E > 30 MeV for the cases in which no EGRET catalogued counterpart source was found for the H.E.S.S. sources. The dashed arrow shows the predicted upper limit from a one-year GLAST scanning observation, taking into account the diffuse emission. Derived from this is the spectral mismatch between GLAST and H.E.S.S. assuming a non-detection with GLAST to illustrate the GLAST will be able to probe the power-law extrapolation from VHE gamma-ray energies whereas the EGRET upper limits are unconstraining in this regard.

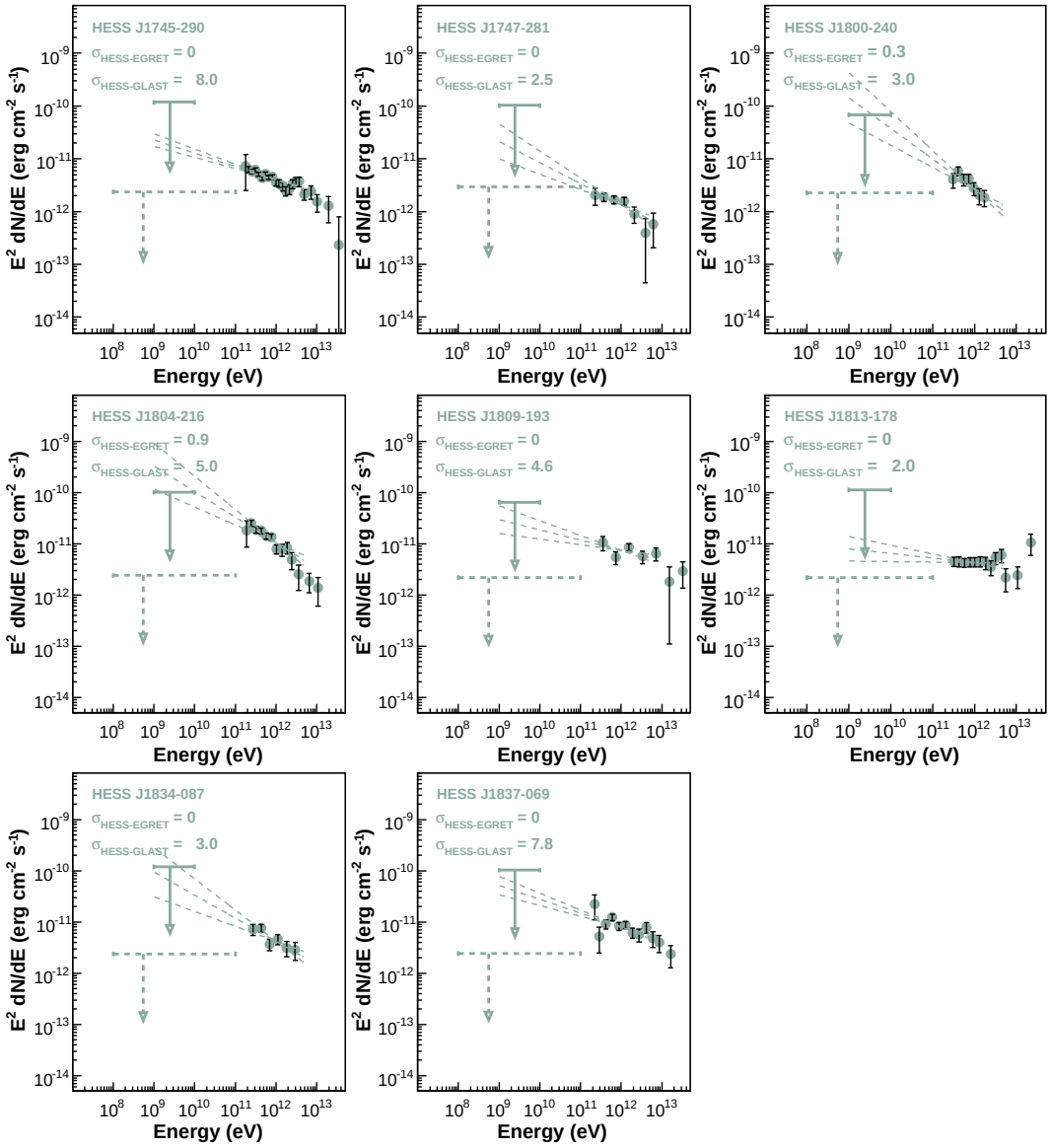

Fig. 8.— (Part 2) Spectral energy distribution at E > 30 MeV for the cases in which no EGRET catalogued counterpart source was found for the H.E.S.S. sources. The dashed arrow shows the predicted upper limit from a one-year GLAST scanning observation, taking into account the diffuse emission. Derived from this is the spectral mismatch between GLAST and H.E.S.S. assuming a non-detection with GLAST to illustrate the GLAST will be able to probe the power-law extrapolation from VHE gamma-ray energies whereas the EGRET upper limits are unconstraining in this regard.

case is that of HESS J1713–395, which was as previously mentioned has been analysed at GeV energies under the assumption that the emission from the source 3EG J1714–3857 is not associated with SNR RX J1713.7–3949. In this case the power-law extrapolation is at the level of the EGRET upper limit and $\sigma_{\mathrm{H.E.S.S.}} = 1$. The unconstraining nature of the EGRET upper limits can be understood by the lack of instrumental sensitivity at GeV energies, which is even worsened in regions of pronounced diffuse gamma-ray emission like the H.E.S.S. GPS region. However, this situation will significantly change in the upcoming future considering the expected sensitivity of the GLAST-LAT as also shown in Figures 7 and 8 in which σ_{GLAST} is calculated for a typical one-year GLAST sensitivity limit in the Inner Galaxy. The numbers suggest that the increased sensitivity of the LAT will predictably elevate such investigation to a level where results will have consequences for the shape of a common emission component at low to high GeV energies. While the EGRET upper limits are currently insensitive for the linear extrapolations of the H.E.S.S. spectra, the GLAST-LAT will predictably allow for more sensitive studies. It should, however, be noted, that a linear extrapolation between H.E.S.S. and GLAST-LAT energies most probably represent a "best-case" for any such study: Real physical models are expected to show spectra that harden towards GeV energies rather than soften, unless a different emission radiation component/process takes over. Concluding this section, at this stage only the number of five connecting cases among the H.E.S.S. and EGRET source in the GPS region can be compared to 17 H.E.S.S. sources where no constraining upper limit at GeV energies could be derived. It remains to be seen if GLAST will pick up emission at comparable or lower energy flux or if the peak in the spectral energy distribution is indeed already made out at VHE energies. As previously discussed, the tremendous advantage of the GLAST-LAT over any previous mission in this context is the continuous energy coverage from 30 MeV all the way up into the VHE gamma-ray range at ~ 300 GeV with significantly improved sensitivity and angular resolution, bridging the current energy gap in which some of the physically interesting suggested energy cutoffs occur.

5. Interpretation

5.1. Sources detected both at GeV and TeV energies

As previously stated and shown in Table 2, only 9 sources exists which we characterise as common Galactic EGRET and VHE gamma-ray sources at this moment (5 within the inner Galaxy, 4 outside of the H.E.S.S. GPS region). Given the large number of Galactic sources in both GeV and TeV gamma-rays this number seems rather low – pointing to different major source classes between the two instruments. However, in particular with respect to

preparations and predictions for the upcoming GLAST mission, there are implications to be made from the connecting cases.

While EGRET and in particular GLAST have sufficiently large fields of view to be able to observe the whole sky, the limited fields of views of imaging VHE gamma-ray instruments (typical FoV: 5°) allows only for rather patchy observations of the whole sky. However, for know GeV sources high-angular resolution VHE instruments such as MAGIC and H.E.S.S. with tremendously higher photon statistics (due to superior detection area) at high energies can help in the identification and interpretation of the GeV emission. This approach has been exemplified by Reimer & Funk (2007) for the Kookaburra complex. In that gamma-ray emission region a re-analysis of the EGRET data taking advantage of the high spatial resolution images from H.E.S.S. observations demonstrated that the dominant GeV emission (3EG J1420–6038) is positionally coincident with HESS J1420–607 (Aharonian et al. 2006c). This EGRET source has been flagged as confused in the 3EG catalogue (Hartman et al. 1999) and in the re-analysis 3EG J1420–6038 was found to be partially overlapping with a less intense second GeV gamma-ray source. This second GeV source – detected below the detection threshold for EGRET – is apparent in a dedicated analysis at approximately 1/3 of the GeV flux of the dominant source (Reimer & Funk 2007) and is positionally coincident with the second VHE gamma-ray source in the Kookaburra region, HESS J1418–609 (Aharonian et al. 2006c) (often referred to as the "Rabbit"). The H.E.S.S. data thus provided a template to separate two overlapping EGRET sources and to even determine the ratio of the gamma-ray fluxes. Studies such as this one show how confused GeV source regions (in particular in the Galactic plane with a dominant diffuse gamma-ray background) might be interpreted by means of connecting the GeV emission as measured from a large-aperture space-based gamma-ray instrument with narrow field-of-view but superior spatial resolution observations by ground-based atmospheric Cherenkov telescopes – a technique that is expected to be very promising for achieving convincing individual source identifications in the era of GLAST-LAT.

On the other hand, the detection of VHE gamma-ray sources with EGRET (or the GLAST-LAT) might help in the interpretation of the TeV data, in particular for the modelling of the gamma-ray emission mechanism. Measuring the energy spectrum of a high-energy gamma-ray source over 5–6 decades in energy should provide rather stringent constraints on the gamma-ray emission mechanism. Unfortunately, the sensitivity mismatch between EGRET and VHE instruments renders this technique presently not as useful as it could be, as shown in Figure 9 for the connecting sources 3EG J1639–4702 and HESS J1640–465 (Aharonian et al. 2006g; Funk et al. 2007). This source shows a rather typical gamma-ray spectral energy distribution exhibiting a power-law spectrum at TeV energies with photon index 2.4 ± 0.15 and a slightly steeper power-law at GeV energies with photon index 2.5 ± 0.18

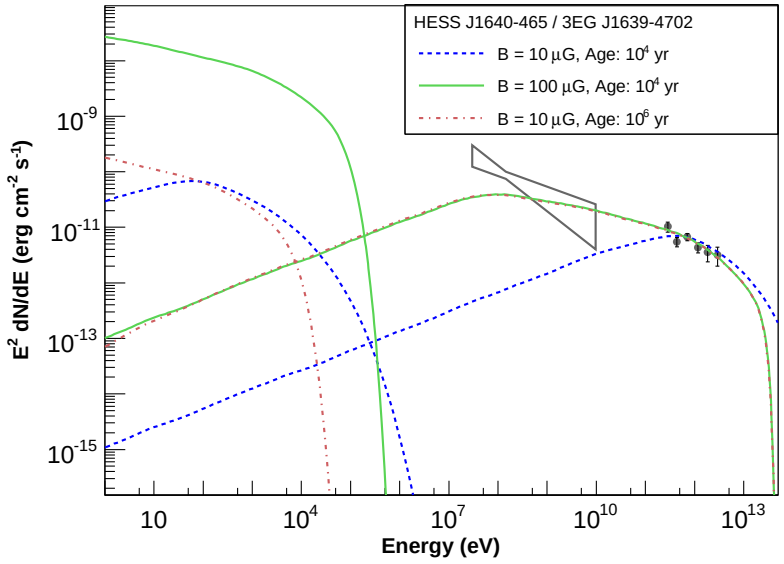

Fig. 9.— Spectral energy distribution for the connecting source HESS J1640-465 along with leptonic IC-models for different magnetic fields and different ages of the system. The purpose of this figure is to demonstrate that rather extreme values for the magnetic-field or the age of the system that have to be invoked to fit such a spectral energy distribution in a leptonic model. These models numerically take into account the time-evolution of the electron spectrum considering energy losses and injection of electrons in time-steps much shorter than the age of the system. Synchrotron and IC losses are calculated following the formalism in Blumenthal & Gould (1970). It should be noted, that the X-ray flux detected from this source is at the level of 10^{-13} erg cm^{-2} s^{-1} as determined by Funk et al. (2007).

at a flux level that is an order of magnitude higher than the TeV flux. The EGRET source 3EG J1639–4702 is with a TS$^{1/2}$-value of 6.4 rather close to the detection threshold and a significantly fainter flux in the GeV band would not have been picked up with the EGRET instrument. Therefore this gamma-ray SED is rather typical for all connecting cases (as also apparent in Figure 3). For a hadronic gamma-ray emission model the shape of this spectral energy distribution can be rather easily reconstructed. For a leptonic IC-model, however, to match the shape of this spectral energy distribution rather extreme values have to be invoked for magnetic field or age of the system. This is demonstrated in Figure 9 which shows 3 leptonic model curves. In the generation of these models, the time-evolution of the electron spectrum due to energy losses was taken into account. These energy losses were calculated according to the formalism described in Blumenthal & Gould (1970). For high energy electrons the energy-loss (cooling) timescale $E/(dE/dt)$ is proportional to $1/E$ for

losses predominantly via synchrotron radiation or IC in the Thomson regime. In this case, for continuous injection of electrons with a power law spectrum $dN/dE \propto E^{-\alpha}$, a spectral break to $E^{-(\alpha+1)}$ will occur. The slope of the IC spectrum (again in the Thomson regime) is given by $\Gamma = (\alpha + 1)/2$. In the idealised case of the Thomson cross-section and a single (thermal) target radiation field the break energy is given approximately by:

$$E_{\rm break} \approx 0.4(t_{\rm source}/10^6{\rm yr})^{-2}((U_{\rm rad} + B^2/8\pi)/1{\rm eV\,cm^{-3}})^{-2}({\rm T}/2.7\,{\rm K})\,{\rm GeV} \qquad (5)$$

In all cases shown here, the time-independent injection spectrum of the electrons was fixed at a photon index of 2.3 and a cutoff energy at 100 TeV, with the IC scattering performed on the cosmic microwave background. The first curve (dashed blue) is derived by using rather typical values for magnetic field (10μG) and age (10^4 years) – that fits the H.E.S.S. data but cannot fit the EGRET data due to the characteristic turnover of the gamma-ray spectrum at lower energies. The other two curves (solid green and dash-dotted red) are shown as illustration how the spectral energy distribution could be accommodated in a leptonic model and thus how the peak of the IC emission can be pushed into the EGRET range. Taking a typical Galactic radiation field (which might not be realistic as e.g. in binary system with a massive stellar component) either rather high magnetic fields (green solid) or rather old sources have to be invoked (dash-dotted red). The high-magnetic field scenario would, however, lead to the prediction of a strongly enhanced high X-ray emission. This prediction violates the faint X-ray flux detected in this object (at the level of 10^{-13} erg cm^{-2} s^{-1}) as well as in most other Galactic VHE gamma-ray sources (where the X-ray emission is typically at the same level or below the VHE gamma-ray energy flux). To explain the gamma-ray emission of connecting sources through IC emission, the sources should thus be rather old to be able to accumulate enough electrons to explain the high GeV flux in a typical Galactic radiation field.

The GLAST-LAT will have about an order of magnitude better sensitivity in the Galactic Plane compared to EGRET and thus the sensitivity mismatch between the LAT and VHE gamma-ray instruments will not be as dramatic. In fact, VHE gamma-ray sources might be detectable by the LAT even if the gamma-ray emission is generated by IC scattering on a typical Galactic radiation field as demonstrated for the Supernova remnant RX J1713.7–3946 where a potential GLAST detection might shed light on the heavily debated origin of the TeV emission (Funk et al. 2007b). Gamma-rays of leptonic origin (produced by IC) might be distinguishable from those of hadronic origin (produced by π^0-decay) through their characteristic spectral shape, although recent claims have been made that under certain conditions the leptonic gamma-ray spectra might resemble those of pionic decays (Ellison et al. 2007). Figure 10 shows that the GLAST-LAT will have the sensitivity to measure energy spectra (in 5 years of scanning observations) for both hadronic and leptonic emission scenarios illustrating that the LAT energy range is particularly well suited to distinguish these models.

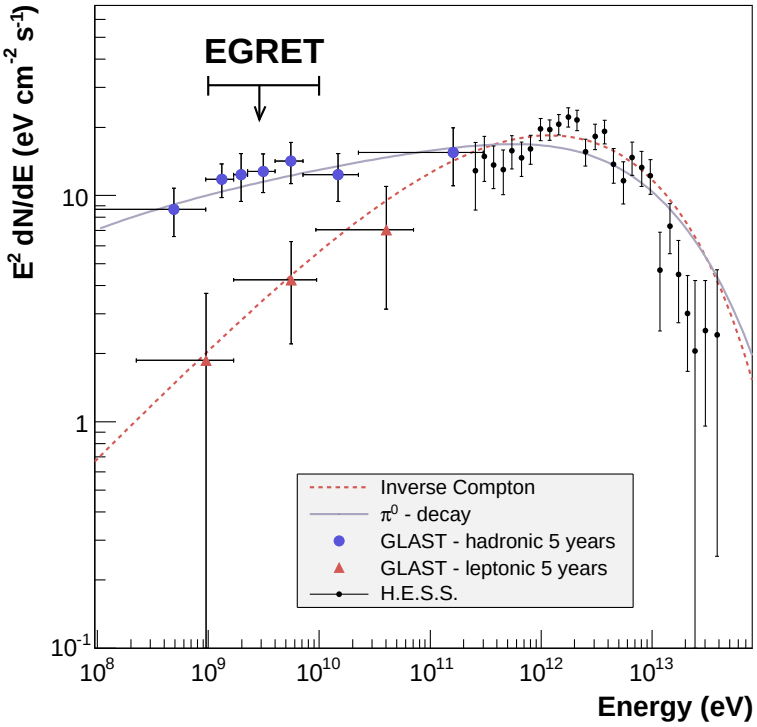

Fig. 10.— High-energy spectral energy distribution for the Supernova remnant RX J1713.7–3946. The black data points denote real measurements with H.E.S.S., whereas the blue circles and red triangles show simulated GLAST data assuming a model for the different mechanisms (leptonic and hadronic) for the γ-ray emission (shown as dashed red and solid blue lines). This simulation uses the current best estimate of the LAT performance and illustrate that in principle the GLAST-LAT should be able to detect this prominent shell-type SNR in a 5-years observation or faster, depending on the exact emission mechanism and therefore extend the energy coverage to GeV energies. This figure has been reproduced from (Funk et al. 2007b).

Measuring the spectral shape of the gamma-ray emission through deep GeV observations with the GLAST-LAT will play an important role in understanding and interpretation of TeV gamma-ray sources.

5.2. The non-connection of GeV and TeV sources

To explain non-connecting cases between GeV and TeV sources various reasons, both caused by instrumental limitations and by physical effects in the source can be invoked as discussed in this section.

5.2.1. Instrumental reasons for non-connection

The most obvious reason for a non-detection of TeV sources with EGRET is the sensitivity mismatch. In a typical ~ 5 hour observation H.E.S.S. is has an energy flux sensitivity of about a factor of $\sim 50 - 80$ larger than EGRET for its entire lifetime above 1 GeV in the Galactic Plane. Additionally, with decreasing detection significance an increasing number of EGRET sources are expected to be artificial, due to peculiarities in the analysis techniques, source confusion in the Galactic plane and in particular due to uncertainties from the model chosen to describe the dominant diffuse gamma-ray emission. As shown in Figure 1, at least the sensitivity mismatch between current GeV and TeV observations (represented by the exposure of the EGRET mission lifetime versus dedicated H.E.S.S. observations) will be alleviated by the upcoming launch of the GLAST-LAT. The LAT will inevitably shed more light on all persistent EGRET sources, since these will be rather bright gamma-ray sources for the LAT instrument. However, it should be noted that the brightest Galactic H.E.S.S. sources (such as RX J1713.7–3946) are not going to be very bright GLAST sources. Detailed simulations using reasonable approximations of the LAT instrument response functions as well as models of the gamma-ray emission in these sources indicates that H.E.S.S. detected Galactic VHE gamma-ray sources will not be the most prominent sources in the GLAST-LAT era (see e.g. Funk et al. (2007b) or Figure 10). Certainly, similar to EGRET, the LAT will (at the lower end of the energy range) suffer from uncertainties and systematic effects due to the analysis technique and the modelling of the diffuse gamma-ray background, however, at a more sensitive flux level.

Another instrumental effect that could render a correlation between GeV and TeV sources unlikely is the insensitivity of imaging VHE gamma-ray instruments towards very extended sources (radius $> 1^\circ$) exhibiting only a shallow maximum. The EGRET data do not put strong constraints on the source extension of a typical point-source in the Galactic plane. Source extensions that can be derived from the data correspond to the EGRET point spread function and are thus on degrees scales. The point spread function and thus the maximum sensitivity of VHE gamma-ray instruments on the other hand is of the order of several arc minutes. The upper limits for H.E.S.S. at the positions of EGRET sources quoted in this study are derived under the assumption of a point-source (with a typical size of the

source region of $\sim 0.1^\circ$ rms width). The sensitivity and thus the upper limit scales roughly linear with the source size (Funk 2005) and for source sizes in excess of $\sim 1^\circ$, the H.E.S.S. data become unconstraining to the problem due to the fact that the source size becomes comparable to the size of the field of view and no reliable background estimations can be performed (see Berge, Funk & Hinton (2007) for a description of the background estimation technique). Large field of view instruments (at however poorer angular resolution) such as Milagro (Atkins et al. 2002) might be better suited to detect sources with intrinsically large sizes in VHE gamma-rays (provided sufficient sensitivity). These instruments suffer, however, from the intrinsic problem of not being able to resolve confused sources. Some of the recently reported Milagro sources indeed seem to line up with EGRET sources (Abdo et al. 2007) and hypothesising that EGRET sources show emission of angular sizes larger than $\sim 1^\circ$, Milagro-type instrument might be better suited to detect large scale gamma-ray emission at VHE gamma-rays. Again, the GLAST-LAT with its superior angular resolution over EGRET will shed more light on the issue of source sizes of GeV sources in the Galactic plane. Naturally, the conclusions derived here are only valid under the assumption that the VHE counterpart to the EGRET emission does not exhibit a size much larger than $\sim 1^\circ$.

5.2.2. Astrophysical reasons for non-connection

The non-detection of most TeV sources in the GeV range by EGRET may be due simply to a lack of instrumental sensitivity. On the other hand, the lack of TeV counterparts to most bright GeV sources requires the presence of steepening (or cut-offs) between 10 and 100 GeV in the spectra of these sources (see section 4 and Figure 6). For these sources that seem to exhibit cutoffs below the VHE gamma-ray range, i.e. in the previously rather unexplored area between 10–100 GeV, the GLAST-LAT will be able to investigate such cutoffs in detail. Steepening in gamma-ray energy spectra between 10 and 100 GeV can occur for many reasons, the most prominent of which are discussed briefly below.

Acceleration limits. The maximum energy to which particles are accelerated in a source may be determined by a balance between the acceleration and energy loss timescales, or between acceleration and escape timescales or simply by the lifetime of the source. In the limit of Bohm diffusion, the escape time of accelerated particles from the source can be written as

$$t_{\rm escape} \sim (r_{\rm source}/{\rm pc})^2 D_0 (E/{\rm TeV})^{-\Delta} \qquad (6)$$

The associated cut-off in the resulting γ-ray emission may occur at much lower energies, as in the case of proton-proton interactions (a factor ~ 20 as shown in (Kappes et al. 2007)), or close to the primary particle energy, as in the case of inverse Compton scattering in the

Klein-Nishina limit (Blumenthal & Gould 1970).

Particle transport may impact on the spectral shape in several ways. For protons described by a power-law $J_p(E_p) = KE_p^{-\Gamma}$ the gamma-rays produced in hadronic interactions are expected to follow a similar power-law spectrum $F_\gamma(E_\gamma) \propto E_\gamma^{-\Gamma}$. Generally, high energy particles escape more easily leading to a cut-off in the particle and hence gamma-ray spectrum inside the source. Therefore, due to particle transport, the spectrum of the protons generating the gamma-rays through hadronic interactions is not necessarily the same as the one at the acceleration site. In the case of diffusion the proton spectrum at the gamma-ray production site can instead be written as $J_p(E_p,\ r,\ t) = \frac{c}{4\pi} f$, where $f(E_p,\ r,\ t)$ is the distribution function of protons at an instant t and distance r from the source. The distribution function satisfies the diffusion equation (Ginzburg & Syrovatskii 1964).

$$\frac{\partial f}{\partial t} = \frac{D(E_p)}{r^2}\frac{\partial}{\partial r} r^2 \frac{\partial f}{\partial r} + \frac{\partial}{\partial E_p}(Pf) + Q, \tag{7}$$

where $P = -dE_p/dt$ is the continuous energy loss rate of the particles, $Q = Q(E_p,\ r,\ t)$ is the source function, and $D(E_p)$ is the diffusion coefficient. Atoyan, Aharonian & Völk (1995) derived a general solution for Equation (7). Hence, as has been emphasised by Aharonian & Atoyan (1996), the observed γ-ray flux can have a significantly different spectrum from that expected from the particle population at the source. In the (expected) case of energy-dependent diffusion ($D \propto E^{-\Delta}$, with Δ typically assumed to lie in the range $\sim 0.3 - 1.0$) the gamma-ray spectrum will follow $F_\gamma(E_\gamma) \propto E_\gamma^{-(\Gamma+\Delta)}$. The exact shape of the spectrum will depend on the age of the accelerator, duration of injection, the diffusion coefficient, and the location of the target material.

The influence of convection (lower energy cutoff in primary particle spectrum) is typically stronger for low energy (GeV) gamma-rays potentially resulting in a VHE gamma-ray source that has no EGRET counterpart in cases in which an external accelerator produces primary hadrons near an active target.Torres, Domingo-Santamaria & Romero (2004) and Domingo-Santamaria & Torres (2006) have recently studied collective wind configurations produced by a number of massive stars, and obtained densities and expansion velocities of the stellar wind gas that is target for hadronic interactions in several examples, showing that these may be sources for GLAST and the TeV instruments in non-uniform ways, i.e., with or without the corresponding counterparts in the other energy band.

Particle energy losses away from the acceleration site may also produce spectral steepening in a very natural way as discussed earlier (see section 5.1). In the case where particle injection is effectively finished (i.e. the injection rate is much lower than in the past), radiative energy losses may produce a rather sharp cut-off in the gamma-ray spectrum as e.g. shown in (Funk et al. 2007). For high energy electrons the energy-loss (cooling) timescale

$E/(dE/dt)$ is proportional to $1/E$ for losses dominantly via synchrotron radiation or IC in the Thomson regime. In this case, for continuous injection of electrons with a power law spectrum $dN/dE \propto E^{-\alpha}$, a spectral break to $E^{-(\alpha+1)}$ will occur. The slope of the IC spectrum (again in the Thomson regime) is given by $\Gamma = (\alpha + 1)/2$. In the idealised case of the Thomson cross-section and a single (thermal) target radiation field the break energy is given approximately by:

$$E_{\rm break} \approx 0.4(t_{\rm source}/10^6{\rm yr})^{-2}((U_{\rm rad} + B^2/8\pi)/1{\rm eV\,cm^{-3}})^{-2}({\rm T}/2.7\,{\rm K})\,{\rm GeV} \quad (8)$$

Gamma-gamma pair-production occurs above a threshold $\epsilon_\gamma \epsilon_{\rm target} > 2m_e^2c^4$. For stellar systems with $\epsilon_{\rm target} \sim 1$ eV, this process occurs above ~ 500 GeV. Pairs produced in gamma-gamma interactions may inverse Compton scatter on the same radiation field - leading to the development of a cascade (Protheroe Mastichiadis & Dermer). Attenuation on the interstellar IR and cosmic microwave backgrounds can be neglected below 10 TeV so gamma-gamma 'cut-offs' are only expected in compact regions of very high radiation density, for example within binary stellar systems. These absorption/cascade 'features' may not represent the end of the gamma-ray spectrum as emission may recover at energies above the resonance.

5.3. Prospects for the GLAST-LAT

As hypothesised in Figures 7 and 8 the GLAST-LAT might indeed be able to detect several of the VHE gamma-ray sources in the inner Galaxy, assuming a simple power-law extrapolation of the spectrum from TeV to GeV energies. While this seems appealing, in a real situation the power-law assumption might not necessarily be a very valid assumption as discussed in the following for various source classes.

Pulsar Wind Nebulae are currently the most abundant VHE gamma-ray sources in the Galactic plane with prominent examples such as the Crab Nebulae (Weekes et al. 1989; Aharonian et al. 2004; Atkins et al. 2003; Aharonian et al. 2006f; Albert et al. 2007a). The spectral energy distribution of PWNe does not readily support a spectral connection even though the Crab Nebula is detected throughout both energy bands. Most VHE gamma-ray PWNe are expected to be dominated by IC emission for which the energy flux generally turns down at lower energies. The position of this inverse Compton peak determines detectability for both GeV and TeV instruments. Also the size of the source and flux level of the emission determines the GLAST-LAT's chances to detect it: The higher the energy of the inverse Compton peak in these sources, the lower the chance to detect them with the GLAST-LAT. If a large fraction of the GeV emission attributed to EGRET Galactic unidentified sources is related to pulsars below the detection threshold, then a correlation between the H.E.S.S.

and EGRET sources in the Inner Galaxy could be expected, given that the majority of the H.E.S.S. sources in this region seem to be PWNe connected to energetic pulsars (Carrigan et al. 2007). However, in reality this expectation might not hold generally due to diversity of parameters like the beaming geometry or different conversion efficiency of the pulsar's spin-down power into the Nebula and into gamma-rays.

Shell-type Supernova remnants The two prominent and bright VHE gamma-ray SNRs (RX J1713.7–3946 and RX J0852.0–4622) are not expected to be very bright GLAST-LAT sources. A detailed simulation of the expected signal from RX J1713.7–3946 shows that it might be detectable in one year of GLAST-LAT observations depending on the assumed TeV gamma-ray emission mechanism as shown in the previous section. Morphological studies in GeV gamma-rays will either have to struggle with moderate angular resolution at low energies or with low photon statistic at high energies. However, spectral studies will be immediately possible following a potential detection as shown in Figure 10. For RX J0852.0–4622 (Vela Junior) the situation is even further complicated by the close-by bright Vela Pulsar. While both of these prominent TeV-emitting objects are rather young ($\sim$ 2000 years), there is the potential of older SNRs acting as stronger GeV emitters (but rather faint TeV sources). In this case the GLAST-LAT might see a different population of shell-type SNRs than VHE gamma-ray instruments, namely older SNRs which have accumulated a lot of lower energy Cosmic rays, but for which the highest energy Cosmic rays that can give rise to TeV emission have already left the acceleration site. A common detection both with GLAST and VHE gamma-ray instruments might require a hadronic origin of the gamma-ray emission rather than an Inverse compton (IC) origin due to the characteristic turn-over in the spectrum at lower energies.

Gamma-ray Binary systems host a variety of non-thermal phenomena. Binaries detected at TeV energies like LS 5039 (Aharonian et al. 2006d), PSR B1259-63 (Aharonian et al. 2005c), LSI +61 303 (Albert et al. 2006) and Cyg X–1 (Albert et al. 2007d) are currently seen as candidates for detection at GeV energies. Gamma-gamma absorption in binary systems can play a role in producing anti-correlation of the TeV to GeV radiation during the orbit of these systems. These orbital modulations are predicted in basically all models for these systems, irrespective of the assumptions of a pulsar or a black hole compact object or the intrinsic scenario and process by which high-energy radiation is emitted (see e.g., (Dermer & Böttcher 2007; Dubus 2006; Paredes, Bosch-Ramon & Romero 2006)). Details in lightcurve and spectral evolution in time are however rather distinctive. Studies including cascading of the pairs through Inverse Compton scattering (Khangulyan, Aharonian & Bosch-Ramon 2007; Sierpowska-Bartosik & Torres 2007) emphasise the anti-correlation, whereas they have also shown detectable GeV properties (both in the spectrum and the light-curve).

6. Summary

When investigating the connection between currently known GeV (EGRET) and VHE gamma-ray sources it is noteworthy that rather few positional coincidences between EGRET and VHE gamma-ray sources are made out for the considered Galactic regions. In addition to positional coincidence, an investigation of the spectral match of the connecting (and non-connecting) sources has been performed based on the assumption of a power-law extrapolation of the spectrum from one energy band to the other. The spectral match was found to be rather good in the case of positionally coincident sources, a property that is not unexpected, given the different sensitivities of the GeV and TeV instruments. Also for the non-connecting cases the sensitivity mismatch might serve to explain why EGRET has not detected many VHE gamma-ray sources, a situation that will dramatically change with the GLAST-LAT instrument in orbit. The sensitivity mismatch can, however, not explain, why VHE instruments such as H.E.S.S. and MAGIC do not detect many EGRET sources. The reason for this must be connected to the fact that a power-law extrapolation from EGRET to TeV energies is in most cases not a valid extrapolation as had been vaguely suggested by previous spectral studies of the brighter EGRET sources discussed here. GeV-cutoffs in the energy spectra of gamma-ray sources can occur for various reasons as discussed above and can render a detection of GeV sources with TeV instruments difficult. Summarising, the study presented here show that the GLAST-LAT will tremendously advance the study of the connection between GeV and TeV sources by bridging the currently uncovered connecting energy range between 10 GeV and 100 GeV. A joint study of a gamma-ray source with GLAST and VHE gamma-ray instruments will provide measurements of the energy spectrum over 5–6 decades in energy and will undoubtedly provide stringent constraints on the gamma-ray emission mechanism in these Galactic particle accelerators.

The authors would like to acknowledge the support of their host institutions. In particular, S.F. acknowledges support of the Department of Energy (DOE) and Stanford University and would like to thank the whole H.E.S.S. and the GLAST-LAT collaborations for their support and helpful discussions on the topic, in particular Werner Hofmann, Felix Aharonian, Benoit Lott, and Seth Digel. DFT is supported by the Spanish MEC grant AYA 2006-00530, he acknowledges Juan Cortina and other members of the MAGIC collaboration for advice and encouragement. OR is supported by the National Aeronautics and Space Administration under contract NAS5-00147 with Stanford University. JAH is supported by an STFC Advanced Fellowship.

REFERENCES

Abdo, A., et al., 2007, ApJ 664, 91

Aharonian F.A., & Atoyan, A.M. 1996, A&A 309, 91

Aharonian, F. A., et al., 2001, A&A 370, 112

Aharonian, F. A., et al. (*HEGRA Collaboration*), 2001, ApJ 614, 897

Aharonian, F. A., et al. (*H.E.S.S. Collaboration*), 2005a, A&A 435, L17

Aharonian, F. A., et al. (*H.E.S.S. Collaboration*), 2005b, Science 307, 1938

Aharonian, F. A., et al. (*H.E.S.S. Collaboration*), 2005c, A&A 442, 1A

Aharonian, F. A., et al. (*H.E.S.S. Collaboration*), 2006a, A&A 449, 223

Aharonian, F. A., et al. (*H.E.S.S. Collaboration*), 2006b, A&A 460, 365

Aharonian, F. A., et al. (*H.E.S.S. Collaboration*), 2006c, A&A 456, 245

Aharonian, F. A., et al. (*H.E.S.S. Collaboration*), 2006d, A&A 460, 743

Aharonian, F. A., et al. (*H.E.S.S. Collaboration*), 2006e, Science 312, 1771

Aharonian, F. A., et al. (*H.E.S.S. Collaboration*), 2006f, A&A 457, 899

Aharonian, F. A., et al. (*H.E.S.S. Collaboration*), 2006g, ApJ 636, 777

Aharonian, F. A., et al. (*H.E.S.S. Collaboration*), 2007a, A&A 464, 235

Aharonian, F. A., et al. (*H.E.S.S. Collaboration*), 2007b, ApJ 661, 236

Aharonian, F. A., et al. (*H.E.S.S. Collaboration*), 2007c, A&A 467, 1075

Albert, J., et al. (*MAGIC Collaboration*), 2006, Science 312, 1771

Albert, J., et al. (*MAGIC Collaboration*), 2007a, submitted to ApJ (astro-ph/0705.3244)

Albert, J., et al. (*MAGIC Collaboration*), 2007b, ApJ 664, 87

Albert, J., et al. (*MAGIC Collaboration*), 2007c, submitted to A&A (astro-ph/0706.4065)

Albert, J., et al. (*MAGIC Collaboration*), 2007d, ApJ 665, 51

Atkins, R. et al., 2002, NIM A 449, 478

Atkins, R., et al., 2003, ApJ 595, 803

Atoyan A. M., Aharonian F. A., & Völk H. J. 1995, Phys. Rev. D 52, 3265

Berge, D., Funk, S. & Hinton, J. A., 2007, A&A 466, 1219

Bertsch, D. L. et al., Proc. 5th Compton Symposium, AIP Conf. Proc. 510, 2000, 504

Blumenthal, G.R., & Gould, R.J., 1970, RvMP., 42, Number 2, 237

Braje, T. M. et al, 2000, ApJ 565, L91

Carrigan, S., et al, 2007, Proc. 30th International Cosmic Ray Conference, Merida, Mexico, 2007

D'Amico, N. et al., 2001, ApJ, 552, L45

Dermer, C. D., & Böttcher, M. 2006, ApJ 644, 409

Domingo-Santamaria E. & Torres D. F. 2006 A&A 448, 613

Dubus G., 2006, A&A 451, 9

Ellison, D. C., et al, 2007, ApJ 661, 879

Esposito, J. A., Hunter, S. D., Kanbach, G., & Sreekumar, P., 1996, ApJ 461, 820

Funk, S., 2005, PhD thesis, Ruprecht-Karls-Universität Heidelberg (http://www.ub.uni-heidelberg.de/archiv/5542)

Funk, S., 2006, ApSS 309, 11

Funk, S., et al., 2007, ApJ 662, 517

Funk, S., et al, 2007b, Proc. 30th International Cosmic Ray Conference, Merida, Mexico, 2007

Gaensler, B. M., et al., 2006, ApJ 648, 1037

Ginzburg V.L., Syrovatskii S.I. 1964, "The Origin of Cosmic Rays", Pergamon Press, London

Hoppe, S., et al, 2007, Proc. 30th International Cosmic Ray Conference, Merida, Mexico, 2007

Hartman, R. C., et al., 1999, ApJS 123, 79

Kappes, A., et al, 2007, ApJ 656, 870

Khangulyan, D., Aharonian, F., & Bosch-Ramon, V., submitted to MNRAS (astro-ph/0707.1689)

Kniffen, D. A., et al., 1997, ApJ 486, 126

Mattox, J. M., et al., 1996, ApJ 461, 396

Mattox, J. M., Hartman, R. C., & Reimer, O., 2001, ApJS 135, 155

Moiseev, A., et al., 2007, APh 27, 339

Nolan, P., et al., 1993, ApJ 409, 697

Paredes, J. M., et al., Science 288, 2340

Paredes, J. M., Bosch-Ramon, V., & Romero, G. E., 2006, A&A 451, 259

Petry, D., 2001, ASSL 267, 299

Protheroe, R. J., Mastichiadis, A., & Dermer, C. D., 1992, Aph 1, 113

Reimer, O. & Bertsch, D.L., Proc. 27th ICRC, 2001, Vol.6, 2546

Reimer, O., & Funk, S., 2007, Ap&SS 309, 203

Romero, G. E., Benaglia, P., & Torres, D. F., 1999, A&A 348, 868

Sierpowska-Bartosik A. & Torres D. F., 2007, submitted to ApJ (astro-ph/0708.0189)

Smith, A., et al, 2007, Proc. 30th International Cosmic Ray Conference, Merida, Mexico, 2007

Sturner, S. J., & Dermer, C. D., 1995, A&A 293 (1), L17

Tavani, M., et al., 1998, ApJ 497, L98

Thompson, D .J. et al., 1994, Nature 359, 615

Thompson, D. J., Bertsch, D. L., O'Neal, R. H., 2005, ApJs 157, 324

Torres, D. F., Romero, G. E., Dame, T. M., Combi, J. A., & Butt, Y. M., 2003, PhR, 382, 303

Torres D. F., Domingo-Santamaria E., & Romero G. E., 2004, ApJ 601, L75

Wang, W., et al., 2005, MNRAS 360, 646

T. C. Weekes et al., 1989, ApJ 342, 379

Zdziarski, A. A., 1987, ApJ 335, 786